Detecting Rearrangements of *Shaker* and NaChBac in Real-Time with Fluorescence Spectroscopy in Patch-Clamped Mammalian Cells

Rikard Blunck,* Dorine M. Starace,* Ana M. Correa,[†] and Francisco Bezanilla*[†][‡]

*Department of Physiology, [†]Department of Anesthesiology, David Geffen School of Medicine, University of California, Los Angeles, California; and [‡]Centro de Estudios Cientificos, Valdivia, Chile

ABSTRACT   Time-resolved fluorescence detection of site-directed probes is a major tool in the investigation of structure-function relationships of voltage-dependent ion channels. However, the technique has been limited so far to the *Xenopus*-oocyte system making it difficult to study proteins, like, e.g., the prokaryotic sodium channel NaChBac, whose expression in oocytes is insufficient or whose physiological functions are distorted in oocytes. To expand the application of site-directed fluorescence detection to these proteins, we used two techniques—semiconfocal epifluorescence and total internal reflection fluorescence—to detect time-resolved fluorescence changes from site-directed labeled proteins expressed in mammalian cells under patch-clamp conditions, and investigated the characteristics and limitations of the techniques. The voltage-sensitive dye, di-8-ANEPPS, was used to monitor control of the membrane voltage in epifluorescence and total internal reflection fluorescence. Fluorescence changes in patch-clamped cells were recorded from a *Shaker* channel mutant (M356C) labeled in the S3–S4 linker using semiconfocal epifluorescence. The gating kinetics and fluorescence changes were in accordance with previous studies using fluorescence spectroscopy in *Xenopus*-oocyte systems. We applied our technique to the prokaryotic sodium channel NaChBac. Voltage-dependent protein-rearrangements of S4 could be detected that are independent of inactivation. Comparison of the S3–S4 linker regions revealed structural differences to the KvAP voltage sensor. The results from the NaChBac channel point to structural requirements for the S3–S4 loop to generate a fluorescence signal.

INTRODUCTION

Local conformational changes of membrane proteins can be detected using time-resolved fluorometric measurements of site-directed labeled proteins (Mannuzzu et al., 1996). The method helps to assign functional processes to specific regions of a protein to elucidate its mechanism and has proven to be a useful tool for understanding the function of voltage-dependent ion channels (Asamoah et al., 2003; Cha et al., 1999a,b; Cha and Bezanilla, 1997, 1998; Chanda and Bezanilla, 2002; Gandhi et al., 2000; Glauner et al., 1999; Mannuzzu and Isacoff, 2000; Smith and Yellen, 2002; Sonnleitner et al., 2002; Sørensen et al., 2000), cyclic-nucleotide gated channels (Zheng and Zagotta, 2000), and several transporters (Geibel et al., 2003a,b; Li et al., 2000; Li and Lester, 2002; Loo et al., 1998; Meinild et al., 2002). Although the operation of ion channels is experimentally detectable as ionic current, the function of many proteins, in contrast, cannot be monitored directly. Dynamic fluorescence measurements also enable the time-resolved observation of the functional processes of such membrane proteins. So far, this technique has been restricted to proteins expressed in oocytes and purified proteins in solution or reconstituted in vesicles.

Although many proteins can be examined with the optical techniques established for oocytes and cell-free systems, some like the prokaryotic sodium channel NaChBac (Ren et al., 2001) require alternative expression systems to achieve sufficient expression levels. Even for those proteins, which can be studied in oocytes, the use of mammalian cell lines is advantageous, since the physiological function of the protein may depend on the expression system. For example, the skeletal sodium channel (Chahine et al., 1994) or NaChBac show abnormally slow inactivation or recovery from inactivation, respectively, when expressed in oocytes. Furthermore, differences in signal transduction pathways in different expression systems can alter interactions of the expressed membrane protein with intracellular cascades. The large diameter of the oocytes reduces the effectiveness of injected dyes and the speed of perfusion systems. In addition, most laboratories have cell culture facilities and established methods of measuring from cell lines, which many researchers are reluctant to deviate from. Hence, establishing a site-directed fluorescence labeling and recording technique in mammalian cells makes it available to study a larger number of membrane proteins.

The much smaller surface area of the mammalian cells relative to frog oocytes leads to reduced signal/noise and signal/background ratios in fluorescence detection. One way to overcome the background staining problem is to insert genetically encoded fluorescent probes (GFP, YFP, CFP) into the protein you want to observe (Riven et al., 2003; Vilardaga et al., 2003; Zheng and Zagotta, 2000). This method, however, has a major disadvantage: the inserted probes can only be attached to peripheral positions, and, since they are fairly large, they are likely to interfere with the movement of the attachment site, making the probe a very

inaccurate mirror of the site's kinetics (Burke et al., 1999; Jugloff et al., 2000). In contrast, the small probes used in site-directed labeling generally do not affect the function of the protein, and can penetrate deeply into the protein (Asamoah et al., 2003; Gandhi et al., 2000). Another disadvantage of using genetically encoded probes is high interfering background fluorescence originating from proteins retained in the endoplasmic reticulum or expressed in various internal organelles (Riven et al., 2003). With membrane-impermeable site-directed dyes one can selectively label externally available sites in proteins expressed in the cell membrane.

In this article, we examined proteins expressed in tissue culture cells using fluorescence spectroscopy. We pursued two techniques to minimize background fluorescence. In total internal reflection (TIR) fluorescence the excitation volume is reduced to a few hundred nanometers normal to the reflection surface (coverslip), therefore exciting exclusively the bottom cell membrane. With semiconfocal epifluorescence (EPI) we reduce excitation and detection volume to decrease the background fluorescence, but keep them large enough to collect the signal from the entire cell at once (for details, see Materials and Methods). We examined whether the two different techniques, TIR and EPI, are appropriate methods for fluorescence detection of voltage-dependent processes. We simultaneously recorded conformational changes of ion channels using semiconfocal epifluorescence and whole-cell patch-clamp recordings in COS-1 cells with high time resolution. The method does not require extremely high expression of ion channels and may be used generally to record protein rearrangements involved in any signal transduction process. Using this technique, movements related to the voltage-dependent gating process of the prokaryotic sodium channel NaChBac was recorded for the first time. We investigated the accessibility of the outer S3–S4 region using fluorescence, and elucidated the role of the S3–S4 linker for the generation of fluorescence signals.

MATERIALS AND METHODS

Chemicals and solutions

All chemicals were purchased from Sigma-Aldrich (St. Louis, MO) or VWR (Cherry Hill, NJ), unless stated otherwise. All solutions for electrophysiology were filtered directly before use.

Depolarizing solution: 150 mM K-MES, 2 mM $CaCl_2$, 20 mM HEPES-Na, pH 7.4. External sodium solution: 140 mM NaCl, 10 mM $CaCl_2$, 5 mM KCl, 10 mM HEPES, 10 mM glucose, pH 7.4. Internal solution: 150 mM KCl, 2 mM $MgCl_2$, 1 mM $CaCl_2$, 2 mM EGTA, 20 mM HEPES, 20 mM sucrose, pH 7.23.

Fluorophores

Tetramethylrhodamine-5'-maleimide (TMRM); di-8-ANEPPS (ANEPPS); Alexa546 maleimide (Alexa546); Alexa647 maleimide (Alexa647); Bodipy FL n-(2-aminoethyl)maleimide (Bodipy); 1-(2-maleimidylethyl)-4-(5-(4-methoxyphenyl)oxazol-2-yl)pyridinium mathanesulfonate (Pympo); and

QSY35 iodoacetamide (QSY35) (Molecular Probes, Eugene, OR). Cyanine 3 monofunctional bihexanoic acid Mono-MTSEA (Cy3); methanethiosulfonate-sulforhodamine (MTSR); (2(5(6) tetramethylrhodamine)-carboxylamido)-ethyl methanethiosulfonate (MTS-TMR); and Texas Red methanethiosulfonate (TxRed) (Toronto Research Chemicals, Toronto, Ontario, Canada).

Molecular biology

M356C-eGFP - (zH4[41eGFP42][M356C]pcDNA3)

eGFP was inserted between residues 41 and 42 of the coding sequence (CDS) of the H4 *Shaker* potassium channel (Schwarz et al., 1988) with the mutation M356C contained in a pCDNA3 (Invitrogen, Carlsbad, CA) expression vector that drives expression in tissue-cultured cells. To insert eGFP into the *Shaker* CDS, a unique BlpI restriction site was introduced silently around residue 41 of the wild type *Shaker* clone, zH4-pCDNA3, by site-directed mutagenesis. The eGFP CDS (Clontech, Palo Alto, CA) (without the stop codon) was amplified by PCR using primers containing linkers to connect in-frame to the BlpI-digested and mung-bean nuclease-treated zH4-pCDNA3 clone. The use of mung-bean nuclease (NEB, Beverly, MA) to shave off sticky ends left by restriction enzyme digestion enabled in-frame insertion of eGFP into the *Shaker* channel without adding extra amino acids.

H4IR-M356C - (H4IR[M356C][W434F]pBSTA)

The nonconducting, inactivation-removed H4 *Shaker* mutant was described in Cha and Bezanilla (1997).

NaChBac - (NaChBac-pTracer)

The wild-type NaChBac-pTracer clone was a kind gift of Dr. Ren (University of Pennsylvania, Philadelphia, PA). Cysteine mutations were introduced in the reported positions using the QuikChange mutagenesis kit (Stratagene, La Jolla, CA).

Transient transfection of tissue-cultured cells

COS-1 cells (ATCC, Manassas, VA) were cultured following standard protocols at 37°C and 5% CO_2 in DMEM + 10% FBS + 2 mM glutamine + 100 units/ml penicillin + 100 μg/ml streptomycin. Cells plated in 24-well plates (10^5 cells/well) were transiently transfected with DNA clones expressing particular channels using Lipofectamine 2000 (Invitrogen). A total of 1 μg DNA mixed with 2 μl Lipofectamine 2000 in 500 μl OptiMem (Invitrogen) was added to each well after media removal. After 4 h incubation the transfection mixture was replaced by fresh medium. The cells were used 18–72 h after transfection.

Cell labeling and preparation

Labeling solution was prepared by mixing a stock solution of dye (50 mM in DMSO) with 20% Pluronic (Molecular Probes) at a ratio of 1:2 and incubated for 5 min before diluting the dye to 50 μM (for MTS dyes) or 5 μm (for maleimide dyes) with depolarizing solution.

Before labeling the cells were incubated 3 min with DTT (50 μM) + EDTA (100 μM) in depolarizing solution to reduce all surface cysteines and to make them available for labeling. After DTT treatment, the cells were washed with Hank's balanced salt solution (HBSS) and incubated for 1–3 min with the respective dye. Excess dye was washed away with phosphate buffered saline (depleted of Ca^{2+} and Mg^{2+}), and the cells were trypsinized and collected. They were washed once in HBSS and resuspended in the respective external recording solution.

Electrophysiology and fluorescence

The setup (Fig. 1 *a*) was mounted on an IM35 (Zeiss, Jena, Germany) inverted fluorescence microscope. A fixed wavelength laser (532 nm, DPGL20, Worldstartech, Toronto, Canada) was used as excitation light source. The light was directed using a multimode fiber (Thorlabs, Newton, NJ) into the lightpath of the microscope using the back port, and could be interrupted by a shutter controlled by the acquisition program via transistor-transistor logic pulses. The laser spot, formed in the focal plane, was defocused to a diameter of 10 μm, so that one entire cell could be excited while the surrounding field of view remained dark. Emitted light was detected with a cooled avalanche photodiode (APD) connected to a Photomax 200 amplifier (Dagan, Minneapolis, MN). The APD could be aligned in *x–y–z* directions with respect to the light spot created by the laser. The light signal was filtered at 1 kHz with an eight-pole Bessel filter and recorded via an ADC board with a PC.

Epifluorescence in semiconfocal mode

In a confocal system a diffraction-limited spot is formed in the focal plane, reducing the excitation volume in the *x–y* plane to a minimum. To reduce the detected volume also in *z*-direction (*z* being the optical axis of the microscope) a pinhole selecting the focal spot in the image plane excludes light originating from a position other than the focal spot. In our setup, we made use of the confocal principle in the *x–y* plane, by reducing the excitation area in the focal plane to the size of a cell, but dispensed, on the other hand, with a pinhole in the detection plane. Therefore, we called this technique *semiconfocal*. The area detected by the APD in the focal plane was 50 μm in diameter. We did not reduce the detection volume any further in *z*-direction, so that we selectively excited all fluorophores on one cell and

collected the entire fluorescence emission from this cell. A further reduction of excitation and/or detection volume would not increase our signal/background ratio but would decrease the intensity of our signal.

The electrophysiological part of the setup was mounted on an aluminum stage that could be moved with 20 nm resolution in *x–y* directions by Inchworm motors (Model 750, Burleigh, Victor, NY) controlled by an ULN6200 controller (Burleigh). The chamber for the cells was positioned over the objective (100×, $NA = 1.25$) of the microscope. The micromanipulators holding the patch-clamp pipette and headstage were mounted on top of the stage, so that the whole configuration (cell, pipette, chamber) could be moved with respect to the laser spot. Electrophysiological signals were processed by an Axopatch 200B patch-clamp amplifier (Axon Instruments, Union City, California) and recorded via the ADC board on the PC. The acquisition and analysis programs were written in-house.

Interchangeable recording chambers were prepared as follows: A centrosymmetric hole was drilled in the bottom of 35-mm petri dishes. A #1 coverslip (for TIR #2, see below) was glued under the bottom of the dish over the hole. For TIR, the rim on the bottom of the dish was removed and, optionally, the internal glass surface was coated with poly-L-lysine (Sigma-Aldrich). When coated, the coverslips were incubated for 1–2 h with 0.01% poly-L-lysine solution in H_2O, rinsed twice with deionized water, and dried in air. The cells were placed in the recording chamber, on the coverslip, shortly before each experiment.

Excitation via total internal reflection

To excite the cells with the evanescent wave of the totally internally reflected beam the setup was adapted similar to the setup described by Sund and Axelrod (2000). In short, using a prism the laser beam was coupled in an appropriate angle into two coverslips sandwiched with immersion oil. The upper coverslip was glued to the bottom of a 35-mm chamber and the cells are placed on this coverslip (see above). We used a 45° prism like Sund and Axelrod but attached its base to the bottom of the coverslip using immersion oil (Fig. 1 *b*). In this way we avoided directing the laser into the prism at a steep angle. A horizontal beam hits the prism at a 45° angle and results automatically in a totally internally reflected beam. The position of the spot where total internal reflection occurs could be adjusted by translating the lens L1 (Fig. 1 *a*) in *x–y* direction. To confirm the correct reflection angle the distance between two reflection spots was verified. In this configuration, fluorophore solution on the coverslip did not show any fluorescence from diffracted beams, indicating total reflection. We used a 60× water immersion objective ($NA = 0.9$, Olympus, Melville, NY) for TIR measurements. Correction for background fluorescence was done by moving the cell out of the detection area and subtracting the remaining fluorescence from all values. The EPI-background fluorescence was negligible, so no correction was done for EPI measurements.

Confocal imaging

For confocal imaging, cells were prepared following the same procedures used for electrophysiological experiments. Images were recorded with a commercially available confocal microscope (Olympus Fluoview/I×70).

Calculation of R_0

The R_0 (equivalent to the distance at which 50% of the fluorescence get transferred to the acceptor/absorber) for the transfer measurements were calculated using
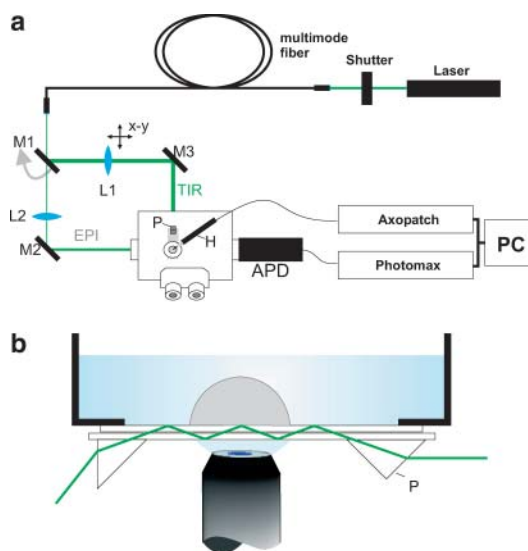

FIGURE 1 Schematic setup. (*a*) Schematic of the optical patch-clamp setup: the laser beam (532 nm) is directed via a multimode fiber to the swiveling mirror (*M1*). M1 was used to select between EPI und TIR fluorescence. For EPI fluorescence the lens (*L2*) was used to adjust the beam size. The beam was directed to the filter cube of the microscope. For TIR fluorescence, the lens (*L1*) was adjustable in *x–y* direction to position a reflection in the center of the field of view. (*b*) A horizontal beam (from *M3*) was directed into a 45° prism. The prism was held with immersion oil on the bottom of the coverslip. If needed, the beam was uncoupled with a second prism on the opposite side of the coverslip (*P*, prism; *H*, headstage).

$$R_0 = 0.211[\kappa^2 n^{-4} Q_D J(\lambda)]^{1/6} (\text{in } \overset{\circ}{A}), \qquad (1)$$

with κ, orientation factor, assumed to be 2/3 (for freely rotating dye); Q_D, quantum yield of the donor in the absence of acceptor; n, refractive index of the surrounding medium; and $J(\lambda)$, normalized overlap integral between donor emission and acceptor absorption (in $nm^4/(cm\ M)$),

$$J(\lambda) = \frac{\int_0^\infty F_D(\lambda)\varepsilon_A(\lambda)\lambda^4\,d\lambda}{\int_0^\infty F_D(\lambda)d\lambda}, \tag{1a}$$

with λ, wavelength; $\varepsilon_A(\lambda)$, extinction coefficient of acceptor at wavelength λ; and $F_D(\lambda)$, fluorescence intensity of donor at wavelength λ (Lakowicz, 1999).

Fluorescence quenching by amino acids

10 ml solutions were mixed from 0.5 M amino acid in buffer (pH = 7.2) and 0.5 M NMG-MES (pH = 7.2), in ratios of 5:0, 4:1, 3:2, 2:3, 1:4, 0:5, and 500 μl TMRM (5 μM), were added. Spectra were taken using an SLM Aminco-Bowman Series 2 luminescence spectrometer (SLM-Aminco Spectronic Instruments, Rochester, NY), with excitation set to 532 nm consistent with the wavelength of the laser in the electrophysiological experiments.

RESULTS

Fluorescence measurements of membrane voltage

We characterized the system properties of fluorescence detection using di-8-ANEPPS, a voltage-sensitive dye, which shifts its excitation and emission spectra as a function of voltage. Using a dye which partitions into the membrane, we become independent from labeling sites or protein expression level. Upon changing the membrane voltage, the normalized EPI fluorescence change (dF/F, Fig. 2 a), which is the difference in fluorescence at both voltages (dF) normalized to the total fluorescence at resting potential (F_1), depended linearly on the size of the voltage pulse (Fig. 2 b). We obtained identical $dF/F = 5\%$ values from oocytes and mammalian cells for a 100 mV voltage pulse ($\lambda_{exc} = 488$ nm; $\lambda_{em} > 515$ nm). With a different choice of emission and excitation wavelengths, the dF/F increased to 10%/100 mV ($\lambda_{exc} = 532$ nm; $\lambda_{em} > 615$ nm). The time response of the
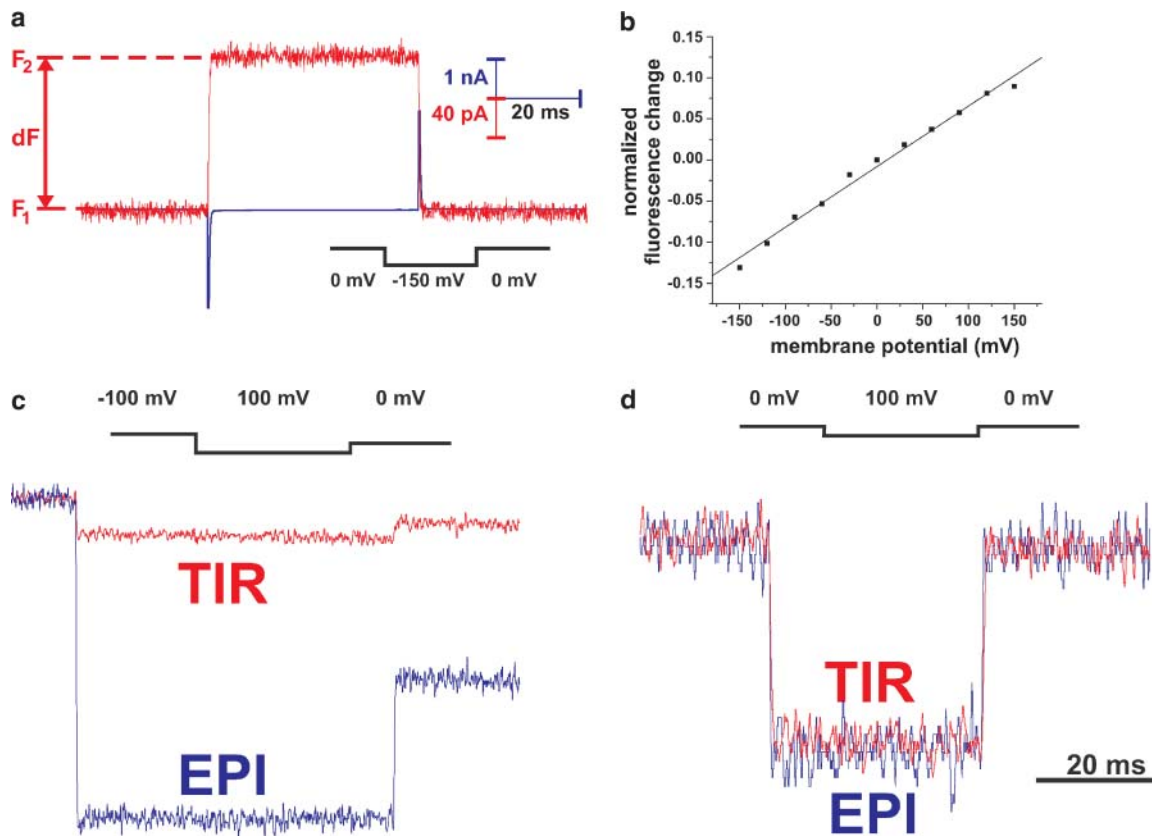

FIGURE 2 Fluorescence detection of membrane voltage. (a) A representative signal (current and EPI fluorescence) for a cell labeled with di-8-ANEPPS is shown. The fluorescence signal (increasing fluorescence for a decreasing step in membrane potential) follows the speed of the clamp since the fluorescence change of di-8-ANEPPS is much faster (Loew, 1982). The fluorescence change dF was normalized to the background fluorescence at resting potential (here 0 mV, F_1). (b) The figure shows the normalized EPI fluorescence changes as a function of the applied voltage pulse. The cell was held at 0 mV and a voltage pulse to the given values was applied. The fluorescence change was normalized to the value at 0 mV. (c–d) Fluorescence response of cells labeled with di-8-ANEPPS excited with TIR or EPI fluorescence. The size of the signal was normalized with respect to the fluorescence at −100 mV (c) or +0 mV (d). (c) Cells were seeded on a clean coverslip. (The protocol was changed to pulse from −100 mV to +100 mV to increase the signal/background ratio in TIR signals.) (d) Cells were seeded on a coverslip coated with poly-L-lysine.

fluorescence signal (Fig. 2 *a*) followed that of the capacitance transient ($\tau_{\text{Fluorescence}}/\tau_{\text{current}} = 1.07$).

Is total internal reflection a suitable method to detect voltage-dependent signals?

Total internal reflection (TIR) (Axelrod et al., 1992) is a very powerful method to reduce the background fluorescence by selectively exciting the plasma membrane. However, background fluorescence arising from dye partitioning into the plasma membrane or from dye binding to other surface proteins cannot be reduced with this method, since these fluorophores will still be excited by the TIR light. For voltage-dependent processes, the use of TIR microscopy introduces another, unique complication: If the access resistance to the outside of the plasma membrane becomes too high due to adherence to the coverslip, it will be impossible to accurately control the membrane voltage. With increasing access resistance, the membrane charging process becomes progressively slower and the membrane potential decreases. This means that membrane regions with medium access resistance slow down the time response and points with high resistance do not show fluorescence changes at all, but only add to the background fluorescence (for details, see Appendix B). Since we wanted to reveal if TIR is suitable for studying voltage-dependent processes, we adapted our setup to enable TIR experiments by changing the excitation pathway as described in Materials and Methods.

We compared the signals detected by EPI and TIR fluorescence (EPIF and TIRF) from untransfected cells labeled with di-8-ANEPPS. Since this dye does not penetrate the membrane, no fluorescence was expected to originate from inside the cell. Hence, exclusively exciting the outer membrane and not the cytosol, like TIR does, will not improve the signal/background ratio compared to EPI. On the other hand, the spot produced by the TIR excitation was elliptical—due to the geometry of the reflection of a beam with finite diameter on the coverslip—and thus larger than the 10 μm circular spot used for EPI fluorescence. Therefore, the unspecific background in relation to the fluorescence signal from the cell was increased when using TIR in comparison to the EPI excitation, which is confined to the area of the cell. The origin of the additional TIR background fluorescence was most likely cell debris on the coverslip or neighboring cells in the detection area, since the bath solution does not significantly add to the background. Thus, we seeded the cells in a low density, so only a single cell was present in the excitation field, and accounted for the remaining background from debris by correcting all fluorescence values for background fluorescence (see Materials and Methods). Fig. 2 *c* shows the time course of the normalized fluorescence of di-8-ANEPPS recorded with EPI and TIR from the same voltage-clamped cell. The ratio of *dF/F*(TIR) to *dF/F*(Epi) was 0.21 ± 0.1 (mean ± SE, *n* = 7; cases where no TIR fluorescence change was detectable were

excluded). Since each value was corrected for background fluorescence, the difference in normalized fluorescence changes cannot solely be explained by background fluorescence differences between TIR and EPI. Furthermore, there was no clear evidence for an increase in the time constant of the fluorescence response, which would indicate areas with medium access resistance. Therefore, the decrease in *dF/F* must be caused by tightly sealing part of the membrane to the coverslip making a very sharp transition between unclamped and well-clamped area. The voltage-dependent signal was detected from those membrane areas, which were far enough away from the coverslip, that their voltage reached its correct value, yet were still close enough to be excited by the evanescent wave. The decrease in TIR-*dF/F* by a factor of 5 suggests that the radius of the unclamped area was 0.45 times the radius of the detected area assuming a homogenous fluorescence distribution (Eq. 3).

Braun and Fromherz (1998) found that there is a 12 nm cleft between a poly-L-lysine-coated surface and the cell membrane. Such a separation should prevent the membrane from sealing to the glass, and the normalized fluorescence change measured with TIR should, depending on the remaining access resistance, either recover to the value measured with EPI or show a slow time constant. After coating the coverslips with poly-L-lysine, the normalized fluorescence changes detected using TIR or EPI fluorescence were identical after correction for background fluorescence (*dF/F*(TIR)/*dF/F*(EPI) = 1.1 ± 0.6, mean ± SE; *n* = 5; Fig. 2 *d*). In addition, the time constants of the fluorescence changes were the same, which suggests that poly-L-lysine coating prevents sealing of the membrane to the glass surface and creates sufficient space to reduce the access resistance and enable proper voltage control. Since our background fluorescence originates mainly from the membrane (see below and Discussion), we used semiconfocal epifluorescence for the following experiments.

Fluorescence changes from *Shaker* potassium channels

To detect fluorescence changes caused by protein rearrangements, cells expressing a *Shaker* channel, M356C-eGFP, containing an eGFP fused into the N-terminal loop (41eGFP42) and a cysteine replacement in the S3–S4 loop at residue 356, were labeled and transferred to the detection chamber. The cells expressing channels were selected by visual inspection for eGFP fluorescence (Fig. 5). The K$^+$ currents of the M356C-eGFP channel show the voltage dependence typical of a *Shaker* K$^+$ channel (Fig. 3 *a*). Fast inactivation due to the N-terminal ball-and-chain mechanism was largely removed, which is most likely because the ball-and-chain mechanism is sterically hindered by the bulky eGFP in the chain, as described earlier (Burke et al., 1999; Jugloff et al., 2000).
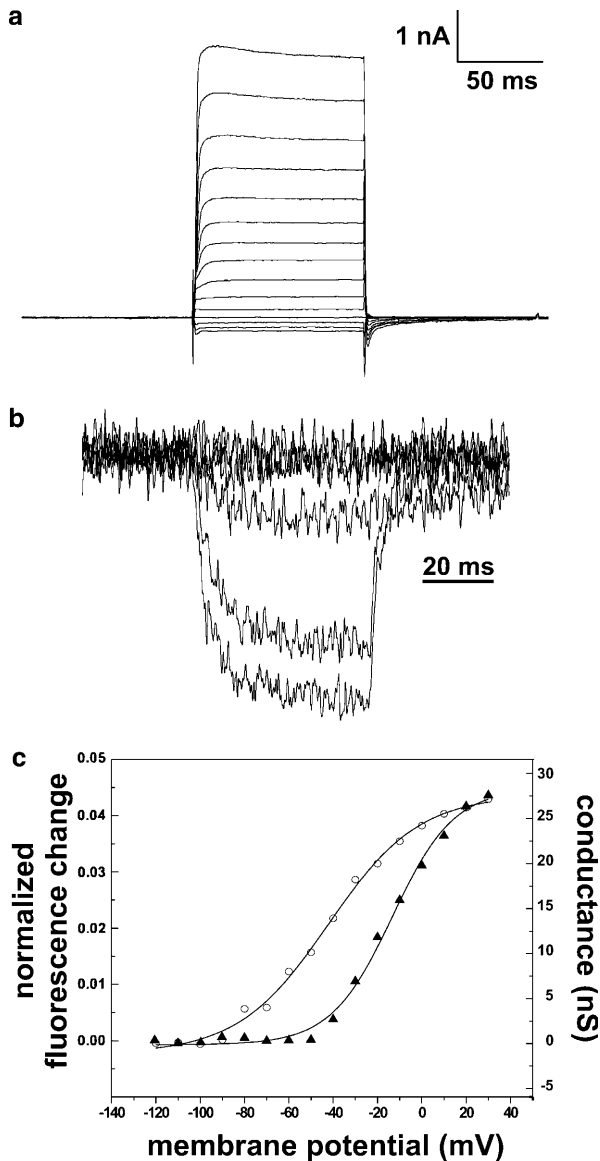
a

1 nA

50 ms

b

20 ms

c

FIGURE 3 Fluorescence changes from *Shaker* channel. (*a*) Currents from a whole-cell patch of cells transfected with the *Shaker* M356C-eGFP channel. The cell was held at −90 mV and pulses from −120 mV to +30 mV in 10-mV increments were applied. (*b*) Fluorescence response of a voltage-clamped cell. The membrane potential was held at −90 mV and pulses from −120 mV to +30 mV in 30-mV increments were applied. Fluorescence decreased upon opening of the channel and the maximum change was detected for the pulse to 30 mV. The whole-cell current was 2 nA. (*c*) Fluorescence-voltage (◯) and conductance-voltage (▲) characteristics for *Shaker* M356C-eGFP labeled with MTSR.

Fig. 3 *b* shows a typical EPI fluorescence signal of a methanethiosulfonate sulforhodamine (MTSR)-labeled cell expressing M356C-eGFP in response to a voltage pulse protocol. The voltage-dependence of the fluorescence changes (*F-V*) and the conductance (*G-V*) were fit to single Boltzmann curves. The fit parameters conveyed a negative 29-mV shift of the *F-V* ($V_{1/2} = -42$ mV) relative to the *G-V* ($V_{1/2} = -13$ mV). The $V_{1/2}$ of the fluorescence changes

corresponds to the $V_{1/2}$ of the gating charge movement ($V_{1/2} = -37$ mV). This confirms that fluorophores attached to the S3–S4 linker of *Shaker* channels report the gating charge movement rather than subsequent pore opening (Cha and Bezanilla, 1997).

The dye has substantial influence on the *dF/F*: methylthiosulfonate versus maleimide linker

Since the main problem for measurements of time-resolved fluorescence changes in mammalian cells is the background fluorescence, we investigated its origin more closely. The measured normalized fluorescence changes, *dF/F*, should decrease with increasing background fluorescence (see Eq. 2). The maximal *dF/F* obtained from M356C-eGFP expressed in COS-1 cells labeled with MTSR was 8.5% with an average of $dF/F = 4.83\% \pm 2.44\%$ ($n = 7$). In cut-open oocyte voltage-clamp recordings a similar value for MTSR-labeled H4IR-M356C channels was measured ($dF/F = 3.22\% \pm 3\%$; max. = 9%).

Empirically we know that for channels expressed in oocytes the best *dF/F* (40%) was achieved using TMR-maleimide (TMRM) to label H4IR-M356C (unpublished results). In contrast, labeling mammalian cells expressing M356C-eGFP with TMRM resulted in enormous background fluorescence. The *dF/F* depended on the channel expression in the cells, and was always <1%. The signal/background ratio is in this case so low because the TMRM penetrates the membrane easily and either labels cytosolic cysteine residues or gets trapped inside the cell or in intracellular vesicles. Confocal images of TMRM-labeled cells revealed labeling of all internal compartments after 1 min of staining time (Fig. 5 *a*). The MTS-linked sulforhodamine MTSR, conversely, did not penetrate the cells (see below and Fig. 5 *b*).

Regardless of the background problem, there is a large discrepancy between the maximum $dF/F = 40\%$ (in oocytes) using TMRM and $dF/F = 9\%$ using MTSR. Cha and Bezanilla (1998) determined that the fluorescence change, *dF*, of TMR attached to position M356 in the *Shaker* channel is due to a quenching mechanism (reduction in fluorescence intensity) rather than a change in the dielectric constant of the surrounding medium (shift of excitation and/or emission spectra), as a result of a transition to a different environment. Two parameters can affect the degree of fluorophore quenching: the overlap between the fluorophore emission spectrum with the quencher absorption spectrum, and the distance between quencher and fluorophore (typically a few Ångstroms for collisional or static quenching, a few nanometers for energy transfer processes). In comparing *dF/F* from TMRM and MTSR, either of the two parameters may be responsible for the difference in the signal: the emission spectrum of TMRM is blue-shifted by 7 nm with respect to the spectrum of MTSR (data not shown) and, due to the

different linkers (MTS vs. maleimide), each fluorophore has a different orientation and distance from the attachment site. To clarify which parameter is decisive for the varying dF, we determined the dF/F of MTS-TMR bound to the M356C-eGFP channel. Note that MTS-TMR is a tetramethylrhodamine fluorophore attached via a carboxylamido bridge to an MTS-reactive group. It, therefore, combines TMR spectral properties with the MTS linker. The MTS-TMR dF/F was determined to be 4.6% ± 1.87%. This value is comparable to the fluorescence change obtained with MTSR but smaller than the dF/F of TMRM at this position, indicating that the altered orientation or distance between quencher and fluorophore is the responsible factor for the reduced fluorescence change at site 356 in *Shaker*.

Increased background in cells is caused by additional external cysteines

Although using MTS-linked dyes reduced the background fluorescence, it remained high and did not differ significantly between untransfected and transfected cells. In comparison, in labeled oocytes there is a threefold increase in background fluorescence, when channels are highly expressed relative to uninjected oocytes. This ratio can be increased if the oocytes are pretreated before surface expression of the channel proteins with nonfluorescent maleimide derivatives to block other cysteine binding sites (Chanda and Bezanilla, 2002; Mannuzzu et al., 1996). Fig. 4 *a* shows the dependence of the MTSR-dF/F on channel expression level. Above 6 nA of current (140/5 mM K$^+$) the dF/F becomes independent of channel expression, suggesting that most fluorescence at this level of expression originates from channel proteins. The decrease in dF/F below 6 nA of current indicates a decreased signal and constant background fluorescence. This background can arise from labeling of cysteines of other membrane proteins, from dye trapped in intracellular compartments, or from dye partitioned into the membrane. For any of these cases it would be challenging to decrease it because it is not only very difficult to reduce unspecific background fluorescence (i.e., non-cysteine-specific), but also to block specific background, originating from labeling cysteines on other proteins, without compromising the desired labeling of the channels and consequently the dF/F. We, therefore, undertook two different approaches to identify the source of the background fluorescence. In the first approach, we increased the number of cysteine binding sites available for labeling by pretreatment with DTT, which reduces oxidized cysteines. Consider two extreme cases: In the first case, if the background fluorescence is caused mainly by unspecific labeling, it will remain unaffected by DTT treatment and the signal/background ratio will increase as more channels sites become available for fluorescent labeling. In the second case, the background is caused mainly by cysteine-specific labeling of other membrane proteins. In this case, new binding sites would become available on these proteins as well as on the channels upon
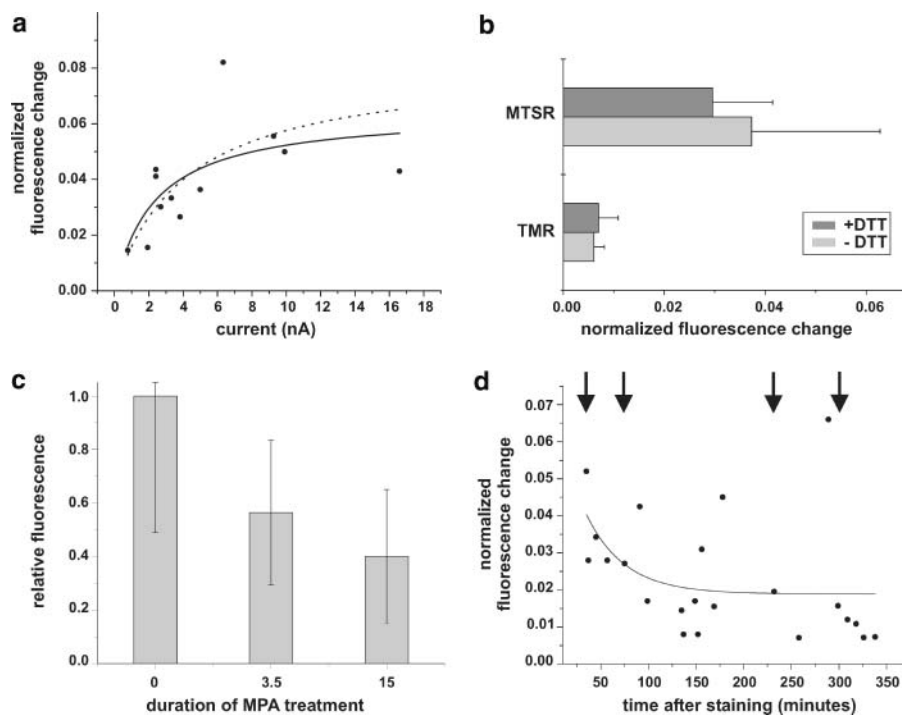

FIGURE 4 Origin of background fluorescence. (*a*) Dependence of normalized fluorescence changes on expression levels of M356C-eGFP in COS-1 cells. The two curves are best fits according to Eq. 2. We assumed that F_{Ch} is proportional to the current. The dotted line has a fixed maximal normalized fluorescence change of 8.5% (best experimental value); the solid line fits the maximal change to 6.7%. Since Eq. 2 requires the background to be constant we only used two sets of experiments with comparable background. (*b*) Effect of DTT pretreatment on the normalized fluorescence change: +DTT cells were pretreated for 3 min with DTT directly before labeling to reduce oxidized labeling sites. −DTT cells were not specially treated. (*c*) Effect of MPA on background fluorescence; cells were incubated in depolarizing solution containing 50 μM MPA for the respective amount of time and then labeled with MTSR. Twenty-five cells were each randomly selected for treated cells and in parallel-labeled untreated cells. The background fluorescence was normalized to the background fluorescence of the untreated cells. No dependence of the background fluorescence on the size of the cells was found. (*d*) Decay of fluorescence change over time; the labeled cells were distributed in four batches and kept in the incubator until used as indicated.

DTT treatment. Assuming that DTT is equally effective in reducing cysteines on channels as on other proteins, the signal/background ratio should remain constant. Pretreating the cells expressing M356C-eGFP with DTT before MTSR-labeling did not change the dF/F significantly although a slight decrease was observed (Fig. 4 b). Cells labeled with TMRM revealed a nonsignificant increase of 16% if pretreated with DTT. Though our results suggest that background is caused mainly by specific labeling of other membrane proteins and that DTT affects channels and background equally, the constant dF/F could also mean that DTT reduced neither the channel proteins nor any other proteins.

In a second approach, to verify that the background fluorescence originates from cysteine-specific labeling, we blocked all available thiol-reactive groups by treating untransfected cells with maleimido propionic acid (MPA, Sigma-Aldrich) (Chanda and Bezanilla, 2002). We could not use this approach with transfected cells to determine a fluorescence change, since the MPA would also block all channel-labeling sites and thereby eliminate any dF. The background fluorescence of 25 cells treated with 10 μM MPA for 3.5 and 15 min and then labeled with MTSR was determined and normalized to the background fluorescence of untreated cells labeled in parallel (Fig. 4 c). The blocking of surface cysteines of untransfected cells clearly reduced the background fluorescence indicating a significant amount of background cysteines on the cells. The results of both approaches, DTT and MPA, suggest that the background fluorescence in mammalian cells originates mainly from specific binding of dye to other membrane proteins.

Internalization of channel proteins decreases signal quality

If after fluorescent staining the cells were returned to the incubator or kept for a short time at room temperature, the dF/F ratio decreased significantly with a time constant of 40 min (Fig. 4 d). Relocation of background fluorophores would not significantly change the background fluorescence, since they contribute equally to the background fluorescence whether expressed on the surface or present in the cytosol. Therefore, the dF/F decay after labeling directly reflects the internalization of the *Shaker* channel proteins. For comparison, Jugloff et al. (2000) determined the mean lifetime on the cell surface of Kv1.4 channels expressed in HEK293 cells to be 125 min. To follow the fate of the MTSR after labeling cells expressing M356C-eGFP, we made confocal images at different time points after labeling. In freshly stained cells the label was found predominantly on the cell membrane, colocalized with the eGFP, indicating the positions of the channels (Fig. 5 b). Nevertheless, some dye could already be observed inside the cells, but it was restricted to vesicles in contrast to TMRM, which was distributed in the cytoplasm (Fig. 5 a). Since the internal
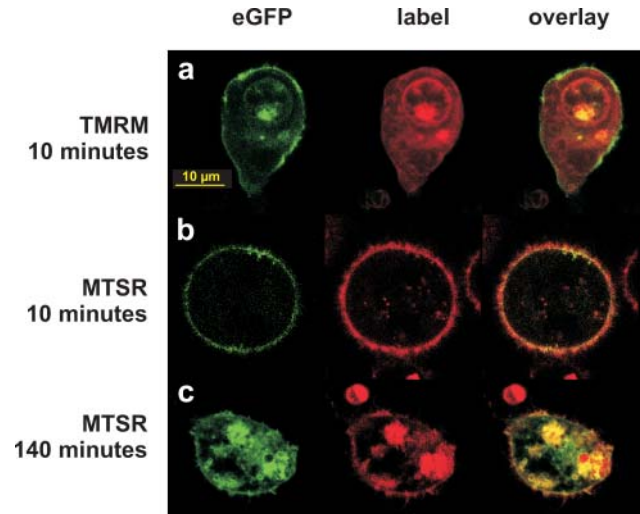

FIGURE 5 Internalization of *Shaker* channels. COS-1 cells expressing *Shaker* M356C-eGFP channels were labeled with TMRM or MTSR and confocal images were taken immediately after and at different times after the labeling. Pictures were taken in the plane where cells displayed the largest diameter. eGFP fluorescence and MTSR/TMRM fluorescence were recorded simultaneously. The eGFP (*left*) displays the position of the channel proteins. (*Center*) MTSR or TMRM fluorescence. (*Right*) The overlay shows how the labeled channels are distributed.

MTSR did not colocalize with the internal eGFP and could also be found in nontransfected cells of the same sample (Fig. 5 b), it could be bound to membrane proteins with fast internalization rates. 140 min after labeling (Fig. 5 c) an increased amount of MTSR was found inside the cell. While for the most part still restricted to vesicles, it was now colocalized with the eGFP, suggesting internalization of the channel proteins. The internalized channels increased the background fluorescence and simultaneously reduced the dF, thus explaining the decay of dF/F with time. To avoid problems caused by internalization of the protein of interest, labeled cells should be kept at low temperature until needed and exchanged frequently.

Voltage-dependent fluorescence changes in NaChBac

To detect gating of the prokaryotic sodium channel, NaChBac, we individually replaced with a cysteine all residues in the outer S3–S4 region between A106 and L118 except F108 and the charged residues (R113, R116). All mutants expressed functional channels with the exception of NaChBac-V109C.

Although labeling cells transfected with the NaChBac mutants with MTSR, which worked nicely in *Shaker*, did not result in a detectable fluorescence change (data not shown), labeling with TxRed and Cy3 showed a voltage-dependent fluorescence change.

The TxRed signal varied significantly in different cells. Closer examination of the TxRed signals revealed that they

indeed consist of two components. Whereas small signals showed saturation ~0 mV, the nicer large signals showed a linear dependence on the membrane voltage (Fig. 6 *a*). The *dF/F* slowly deviates from the linear behavior when pulsing to voltages more positive than −20 mV. Fig. 6 *b* shows time traces of TxRed fluorescence bound to NaChBac-L112C. The signal here seems to saturate at depolarized potentials. Unfortunately, we could not conclusively remove the linear component from the TxRed signal. Untransfected cells also showed a small signal that was linear over the entire voltage range. The fact that the signal did not change with different emission filters (610LP over 610/40BP) indicates that the signal is not electrochromic. Most likely it originates from dye bound to endogenous proteins or dye partitioned into the membrane. Since we could not remove the linear component from the TxRed signal, we changed to Cy3, which gives a smaller but saturable signal.

At all positions tested in NaChBac the fluorescence changes obtained were very small even with high expression (4 nA in 70 mM Na$^+$) equivalent to *Shaker*-M356 (see above). The fluorescence time traces shown in Fig. 7 *a* are obtained from Cy3 bound to NaChBac-L115C. The maximal *dF/F* obtained was 0.41%. Although the signal is clearly visible, the signal/noise ratio is too low to allow reliable extraction of information about the gating kinetics of NaChBac. Nevertheless, it becomes obvious that the movement reported for by the Cy3 fluorescence does not follow the inactivation kinetics of NaChBac, but remains in the depolarized position until repolarization. This indicates that the dye attached to the S4 helix is connected to the movement of the voltage sensor leading to activation and is not related to inactivation.

Fluorescence scanning of S3–S4 linker region

Alignment of the S3b–S4 region of KvAP and NaChBac with other voltage-dependent channels reveals differences in this region between these two prokaryotic channels (Fig. 8). The elsewhere conserved proline in S3 is missing in NaChBac; instead a glycine is present on position G100. In KvAP, in contrast, two prolines (P95 and P99) pre-

sumably break the S3 helix into two parts (Jiang et al., 2003a). According to the crystal structure (Jiang et al., 2003a), the helical structure of the S3 extends longer into the S3–S4 linker than predicted in the literature for other channels (Fig. 8). In *Shaker*, a longer S3 helix is supported by deletion experiments by Gonzalez et al. (2001), demonstrating that the S3 and S4 helices extend into the putative linker region. However, if the NaChBac S3-helix structure were analogous to the KvAP crystal structure up to position L112 (corresponding to G112 in KvAP), the S3 and S4 (S4 starts at the leucine or phenylalanine right before the first charge of the voltage sensor) would fuse directly into each other with no linker at all. Obviously, an extended helix is therefore not possible in the prokaryotic NaChBac. Looking at the crystal structure of the isolated voltage sensor attached to FaB-fragments (Jiang et al., 2003a), it seems that there is not much play between S3 and S4 in KvAP, since the linker is very short. If, on the other hand, the coordination of the charged residues E93 and the arginines in S4 is analogous in both channels (Fig. 8), the NaChBac S3 helix does not consist of sufficient amino acids to build up the backbone. In the KvAP structure L110 is very close to L115. It is, therefore, plausible that in NaChBac, the S3 helix consists of one turn less and NaChBac-V111 is equivalent to KvAP-L115 while NaChBac-T110 is equivalent to KvAP-L110. The very tight coupling of S3 and S4 in this case would impose a concerted movement of S3 and S4.

One consequence from the tight coupling of S3 and S4 is that the extracellular region becomes more compressed compared to the *Shaker* channel and accessibility of the residues may become blocked. We addressed this question, by studying accessibility of the outer S3 and S4 region with fluorescence. Fig. 9 shows the normalized fluorescence change (*dF/F*) of Cy3 attached to the cysteine at indicated positions. One can deduce from the fluorescence change the extracellular accessibility of the attachment sites (Gandhi et al., 2003). It is interesting that the signals from the deepest residues A106 and L118 are largest, whereas the neighboring residues Q107 and V117 do not give any signal. This is consistent with the fact that fluorophores attached to the accessible residues further inside the protein make more
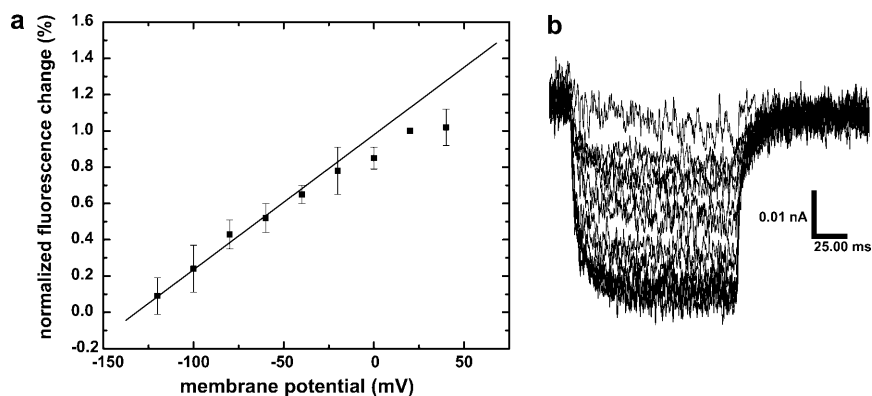

FIGURE 6 Fluorescence changes from NaCh-Bac-L112C. Cells were labeled with TxRed. Excitation wavelength was 532 nm and emission was filtered using a 610-nm longpass filter. (*a*) Normalized fluorescence change as a function of membrane potential. Voltage pulses from −150 mV to the indicated voltage were applied. (*b*) Fluorescence versus time traces of cells labeled with TxRed. Pulses from −150 mV to voltages ranging from −120 mV to +80 mV in 20-mV steps were applied.
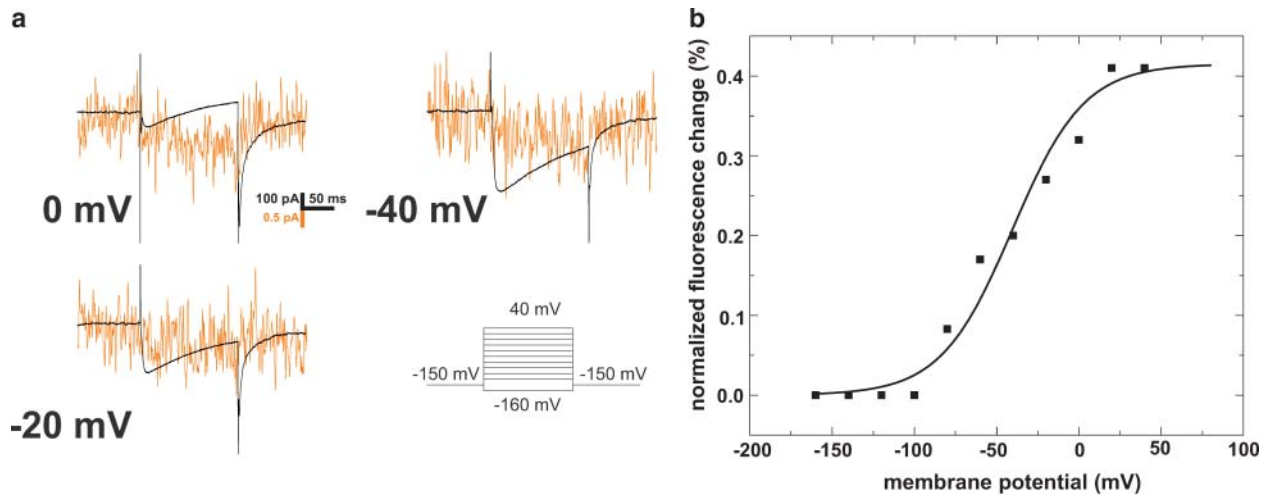
FIGURE 7   Fluorescence changes from NaChBac-L115C. Cells were labeled with Cy3. Excitation wavelength was 532 nm and emission was filtered using a 610/75-nm bandpass filter. (*a*) Fluorescence and current versus time traces of cells during depolarizing pulses to the voltages indicated. Voltage protocol was applied as shown. (*b*) Normalized fluorescence changes as a function of membrane potential. Voltage protocol was applied as in *a*.

contact to the surrounding residues, so that a fluorescence change is more likely. However, the deeper a residue is buried within the channel protein, the higher is the chance that they will not be accessible unless waterfilled crevices reach their position. L112C probably only gives a very small signal because this residue is too exposed. L112C is on the far top of the S4 segment and a dye attached to it may not make contact with any other residue (see below). Although this could be the case for Q107 and V117, it seems unlikely, since these residues are comparably deeper into the protein. These residues may be directed toward surrounding helices and thus not accessible to the dye. In summary, most residues down to the third charge in S4 (R119) and on the outer S3 are accessible to labeling with Cy3. This result is in agreement to accessibility studies in *Shaker* (Larsson et al., 1996).

The S4 segments do not undergo a large movement relative to each other

The above discussion would support formation of a complex (paddle) as the voltage sensor in KvAP and NaChBac. Jiang et al. (2003b) suggest a large movement of the paddles consisting of S3b and S4 of KvAP as a consequence of voltage changes. If the outer positions of the voltage sensor undergo a considerable distance change during gating, this should be detectable using resonance energy transfer. We used the absorber QSY35-iodoacetamide (Molecular Probes) as an acceptor in combination with Alexa546 or MTS-TMR as donors since the R_0 (the distances at which half the donor fluorescence is transferred to the acceptor/absorber) are 22 Å for Alexa546 and 21 Å for MTS-TMR, close to the putative distance of two neighboring S4 segments in *Shaker* (28-32 Å) (Blaustein et al., 2000; Cha et al., 1999b). Labeling NaChBac with a 1:1 mixture of Alexa546 or MTS-TMR with the absorber QSY35 revealed a small voltage-dependent signal. The fluorescence change was too small ($<0.25\%$) to define a distance or movement of the S4 segments relative to each other. A fluorophore-fluorophore pair with longer $R_0 = 42$ Å (Bodipy and Alexa647) did not show a voltage-dependent signal. The very small or nonexistent signals indicate that there is a very small distance change of the outer regions of the S4 segments relative to each other in NaChBac.

FIGURE 8   Sequence alignment of several voltage-dependent channels. The anionic group and proline in S3 as well as the positively charged residues in S4 were used for alignment. The boxes indicate the putative helices (S3 and S4) as reported before (Gonzalez et al., 2000; Jiang et al., 2003a; Ren et al., 2001; Shoeb et al., 2003; Tang and Papazian, 1997). Comparison of the helices in KvAP taken from the crystal structure and NaChBac reveals that the helical regions are different. In the other channels a further extension of the helices into the linker is possible.
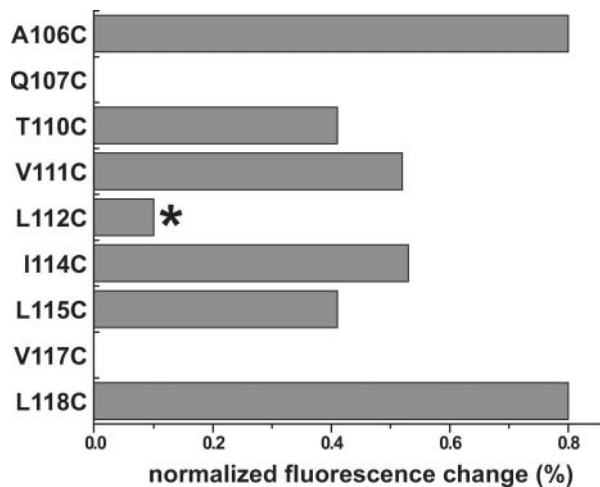
FIGURE 9 Fluorescence scanning of the S3–S4 linker region of NaChBac. Maximal normalized fluorescence change obtained from Cy3 attached to the indicated positions in NaChBac. NaChBac-L112C could not be determined exactly because of low signal/noise ratio.

The characteristics of the S3–S4 linker are decisive for fluorescence signal

The relative fluorescence change signals obtained from NaChBac are much smaller than the signals obtained from analogous positions in *Shaker*. Moreover, in *Shaker* almost all analogous positions show a reasonable-sized fluorescence signal with different dyes in oocytes (Asamoah et al., 2003; Cha and Bezanilla, 1997; Gandhi et al., 2000).

Table 1 summarizes all the positions where a voltage-dependent fluorescence change could be detected with a variety of dyes. It becomes immediately obvious that the dye MTSR, which resulted in a large voltage-dependent fluorescence change in *Shaker*, did not give any voltage-dependent signal in NaChBac. Also Alexa546 and Pympo did not generate detectable signals from NaChBac. Only the fluorescence of the two dyes Cy3 and TxRed consistently changed in a voltage-dependent manner. We think it would

TABLE 1 Summary of fluorescence signals from different positions in NaChBac; positions in parentheses indicate that the signal is very small

Dye	Positions with fluorescence change	Positions with no fluorescence change
Cy3	A106, T110, V111, (L112), I114, L115, L118	Q107, V117
MTSR		V111, L112, I114 V117, L118
Pympo		L112
TxRed	T110, V111, L112, I114	
Alexa546 + QSY35	L112, L115	
MTS-TMR + QSY35	(L112), L115	
Bodipy + Alexa647		L112

be quite informative to explain the differences in the magnitude of the fluorescence signals between NaChBac and other channels studied. Table 2 compares signals obtained from the S3–S4 linker of different voltage-dependent channels along with the length and composition of their linker. It is apparent that the relative fluorescence change is not only dependent on the attachment site of the dye in the channels, but also on the surrounding structure of the protein. The magnitude of the signal may depend on the protein structure because the fluorophore can be quenched by surrounding amino acids (aa) or transferred from a hydrophobic to a hydrophilic environment. In the case of the *Shaker* channel, Cha and Bezanilla (1998) showed that the signal originated from a change in quenching rather than change in hydrophobicity. The *Shaker* channel has by far the longest linker (30 aa) and generates the largest signal. The EAG channel still results in large dF/F (13%) and, accordingly, has a relatively large linker (13 aa) (Schonherr et al., 2002). Very short linkers are found in MaxiK (hSlo) (5 aa) and NaChBac (2 aa). Both channels only generate very small signals. Fluorescence changes in Herg channels are intermediate (Smith and Yellen, 2002) though the linker has almost the same length (9 aa) as EAG (13 aa). It stands to reason that not only the length of the linker is important for the generation of a fluorescence signal, but also its aa composition. Sørensen et al. (2000) found that the fluorescence change originating from *Shaker* in S3–S4 at M356C is pH-titratable and suggested that the motif EEED (positions 333–336) may be responsible for the fluorophore quenching. In fact, they could demonstrate that the dF/F is diminished 10-fold by deleting all except the last five residues of the S3–S4 linker, which included EEED (Δ330–355). Table 2 shows also that EAG has a motif EXXDE in the start of the S3–S4 linker and exhibits a large dF/F. In Herg, on the other hand, the motif EE is located right next to the TMR attachment site, so that there will not be a large relative movement between fluorophore and the EE. The reason for the smaller signal in Herg may hence be the close proximity of the TMR attachment site to the glutamates in the linker.

We tested the ability of glutamate and aspartate to quench TMR. Fig. 10 *a* shows the emission spectra of TMRM in solution with increasing concentrations of glutamate. At 500 mM the fluorescence intensity was significantly reduced (35%), with no detectable shift in the emission spectrum with regard to glutamate-free solutions. An equal concentration of aspartate, in comparison, only quenches TMR fluorescence by 11% (Fig. 10 *b*). Glycine, surprisingly, increases TMR fluorescence (40%). The high quenching efficiency of glutamate supports the idea that glutamate, and partly aspartate, are responsible for the quenching in the *Shaker* EEED motif. We conclude that the very short linker in the prokaryotic channels KvAP and NaChBac (as well as in MaxiK) and the lack of quenching residues in the surrounding amino acids may explain the small size of the fluorescence signal of NaChBac.

TABLE 2 Sequence comparison of different S3–S4 linkers of voltage-dependent ion channels

Channel	Literature	S3 end	Linker	S4 start	Linker length	dF/F
Shaker	Cha and Bezanilla (1998)	T329	VVA**EEEED**TLNLPKAPVSPQ**D**KSSNQA<u>M</u>SL<u>A</u>	I360	30	25%
Shaker Δ330–355	Sørensen et al. (2000)	T329	A<u>M</u>SL<u>A</u>	I360	5	1–2%
EAG1	Schonherr et al. (2002)	F312	**E**NV**DE**GISSLFSS	A325	13	13%
HERG	Smith and Yellen (2002)	F515	GSGS**EE**L<u>I</u>G	L525	9	3%
hSLO	R. Olcese (personal comm.)	L199	NR<u>S</u>WL	G205	5	<1%
NaChBac		T110		V111	0	<1%*
KvAP		G112	LG	L115	2	—

See Fig. 8. The start of S4 was set independent of the literature to two amino acids before the first charge, *R* or *K*, in S4. Anionic amino acids are printed in bold, and the attachment sites of the probes are underlined. *dF/F* shows the maximal relative fluorescence change measured at that site according to literature. *Indicates that these measurements were obtained from cells, in contrast to the rest, which were obtained from oocytes.

DISCUSSION

Detecting fluorescence changes from mammalian cells

In this study, we presented two techniques to detect fast fluorescence changes from patch-clamped mammalian cells: semiconfocal epifluorescence and total internal reflection. When observing protein rearrangements in patch-clamped cells, one encounters signal/noise and signal/background challenges. These were not noted in the frog oocytes system since the ratio of surface/detection volume is very favorable. Therefore, we tested two different ways to overcome these obstacles. With semiconfocal epifluorescence the signal/background ratio was improved by selecting the excitation and detection volume according to the size of one cell, and with TIR fluorescence by preferably exciting the bottom membrane of the cells. While with both methods, TIRF and EPIF, fluorescence changes from the voltage-sensitive dye di-8-ANEPPS could be detected, for TIR fluorescence the glass surface had to be coated with poly-L-lysine to maintain sufficient access to the bottom membrane for proper voltage control. When using TIR, one must also consider eventual inhomogeneous distribution of membrane proteins or difficult access for introduced ligands. Because TIR restricts the excitation volume to the membrane and distinguishes between surface and cytosol, it is preferable in cases of high background originating from inside the cells. This could result from internal labeling as well as from retained or premature proteins fused to genetically encoded fluorophores. Our results indicate that when using membrane-impermeant dyes most of the background fluorescence is due to labeling of other surface proteins, which cannot be separated from the channels by using TIR excitation. Therefore, TIRF offers no advantage over EPIF in this case. EPIF, on the other hand, has the advantage that the circular excitation spot is reduced to the size of the cell and for that reason does not excite extra background on the coverslip's surface. Furthermore, the light penetrates the entire cell, so that the excited surface is larger, increasing the signal intensity.

Hence, we used the semiconfocal epifluorescence technique for detection of conformational changes during voltage gating. We found that the signal/background ratio is dependent on the level of protein expression (Fig. 4 *a*). To
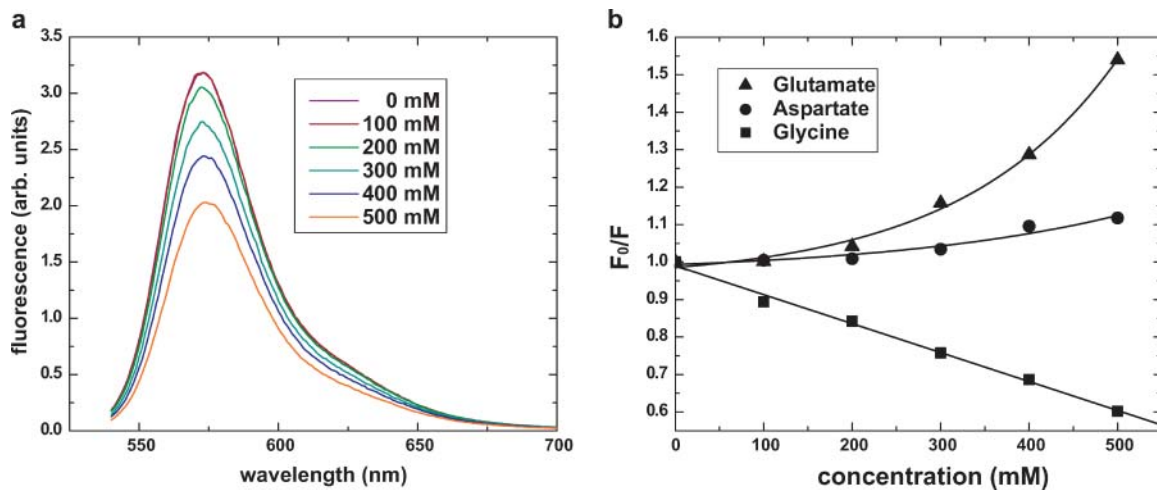

FIGURE 10 Quenching and unquenching of TMR fluorescence with glutamate, aspartate, and glycine. (*a*) Emission spectra of glutamate in solution. Excitation wavelength was 532 nm. (*b*) F_0 is the fluorescence in the absence of the quencher; *F* is the fluorescence at given concentration. Excitation wavelength was 532 nm.

further improve the signal/background ratio, selective excitation of the desired proteins by resonance energy transfer should be applied. In the case of homotetrameric ion channels, one can make use of the fourfold symmetry of the protein and label with a mixture of one donor and acceptor dye each (Cha et al., 1999b; Glauner et al., 1999).

One of the major problems for fluorescence detection in mammalian cells is penetration of the cell membrane by many conventional dyes. When this problem occurs in oocytes it is significantly reduced by melanin below the cell membrane that shields the background fluorescence from inside. We found that MTS-linked dyes did not enter mammalian cells, suggesting that in the case of TMR the hydrophobic maleimide group is responsible for its permeation. Penetration of TMRM into the cell could, on the other hand, be used for internal site labeling.

Coordination of fluorophore and quenching groups

On the other hand, the linker in the fluorophore has another important influence: in the *Shaker* K$^+$ channel, labeling with MTS-TMR exhibited a reduced normalized fluorescence change (*dF/F*) compared to TMR-maleimide (TMRM). Since the fluorescence spectra of MTS-TMR and TMRM are identical, this decrease in *dF/F* is most likely caused by a different orientation and/or distance of the fluorophore relative to a quenching group.

In the *Shaker* channel, the quenching groups responsible for the fluorescence signals from the region of the voltage sensor are particularly well coordinated, since most positions in the outer S4 can be probed by fluorescence changes (Asamoah et al., 2003; Cha and Bezanilla, 1997; Gandhi et al., 2000). Our measurements from the homologous region of the prokaryotic sodium channel, NaChBac, demonstrate that analogous quenchers are missing in this protein. Comparison with different voltage-dependent ion channels reveal that the length and composition of the S3–S4 linker seems to be a major player in recorded fluorescence signals. A longer linker, as in the case of the *Shaker* channel, and anionic amino acids, primarily glutamates, are required for quenching of the fluorophore. Also important are the relative positions of the glutamates with respect to the fluorophore, enabling the mutual interaction necessary for conformation-dependent quenching. The prokaryotic NaChBac as well as the MaxiK channel have neither a long linker nor any anionic residues in the linker region, and both show very small signals during depolarization.

Voltage-dependent fluorescence changes from NaChBac

The signals obtained from NaChBac were very small, so that little information about the gating kinetics could be extracted. Nevertheless, in NaChBac it was found that the movement reported by the Cy3 (and TxRed) fluorescence changes follows the activation but not the inactivation kinetics of the channels. The fluorescence seems to remain in the depolarized position even after inactivation has developed and it does not return until the voltage is repolarized.

Sequence alignment of the two prokaryotic channels NaChBac and KvAP (Fig. 8) revealed that, despite high sequence homology, there are structural differences in this region between the two channels. The lack of four amino acids in the S3 of NaChBac can be resolved if the S3-helix of NaChBac consists of one turn less than S3(b) of KvAP. The accessibility down to the third charge of S4 (R119) is not compromised by the very short linker of NaChBac. But the very short linker in these prokaryotic channels supports the idea of S3 and S4 acting together in a concerted manner as the voltage sensor, as Jiang et al. (2003a) hypothesized based on the crystal structure. In *Shaker* K$^+$ channels the situation seems quite different. Here, the linker has a considerable length, so that a tight connection between the S3 and S4 is not compulsory. Mathur et al. (1997) showed that the short *Shab* or *Shaw* (but not *Shal*) S3–S4 linker, transferred into a *Shaker* background, slows down the activation and deactivation kinetics, and Gonzalez et al. (2000) demonstrated a periodic dependence of the activation time on the linker length with very short linkers.

The fluorescence measurements in NaChBac suggest that the structure of its voltage sensor is similar to the KvAP voltage sensor structure, but they do not support large conformational changes during voltage sensing. The present study also points to functional differences of their voltage sensor with regard to the voltage sensor of the *Shaker* channel. These differences between *Shaker* and the prokaryotic channels make clear how important it is to understand the gating mechanisms of prokaryotic ion channels and to establish their structure-function relationships. Prokaryotic ion channels are particularly amenable to other structural and functional techniques such as biochemical purification, bilayer reconstitution, and crystallization, giving a full complement of structure and function studies not yet possible in eukaryotic channels. Since NaChBac does not sufficiently express in oocytes, it has not yet been possible to record its gating process with fluorescence techniques. The technique presented here has allowed us to detect conformational changes during gating with moderate levels of expression. Further improvements of the signal/noise ratio by, e.g., directed mutagenesis should help us understand the conformational changes and gating kinetics of this prokaryotic channel.

APPENDIX A: INFLUENCE OF BACKGROUND ON MEASURED *dF/F*

Let

dF = Fluorescence change measured upon opening of the channels.
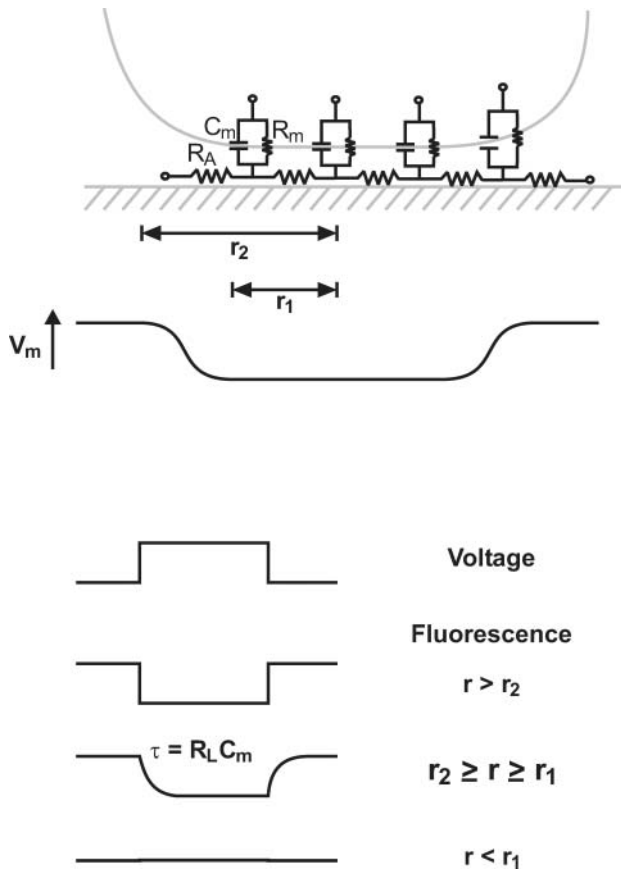
FIGURE 11 The TIR problem—voltage control and fluorescence detection. The system of the cell sitting on a glass surface corresponds to a cable problem. Each patch of membrane has a membrane capacitance C_m and a membrane resistance R_m as well as an access resistance R_A. The access resistance is a function of the surrounding membrane patches and the distance between the cell and the glass surface. We assume that within the radius r_1 from the center of the cell, the access resistance is very high, and thus most of the applied voltage drops over the lumped access resistor R_L. In this case the membrane potential V_m is very low. Within the region $r_2 \geq r \geq r_1$, the access resistance decreases (the cell does not seal to the glass, the access resistance is dependent on the distance). The voltage will increase depending on the ratio R_L/R_m. Nevertheless, the expected time course of the voltage as a response to a voltage step in this region will be dependent on the time needed to charge the capacitance C_m. This time course will be convoluted with the fluorescence response we are measuring. Key: r_1, radius of sealing area; r_2, radius with medium access resistance; and r_{det}, radius of detection area (excitation with evanescent wave).

F_{Ch} = Fluorescence originating from fluorophores bound to channels (in the resting state).

F_P = Fluorescence originating from fluorophores bound to other proteins.

F_B = Fluorescence originating from nonspecifically bound fluorophores.

F = Total fluorescence ($= F_{Ch} + F_P + F_B$).

Dependence of *dF/F* on background fluorescence

The experimentally determined fluorescence change is

$$\frac{dF}{F} = \frac{dF}{F_{Ch}} \times \frac{F_{Ch}}{F_{Ch} + F_P + F_B}, \qquad (2)$$

where dF/F_{Ch} is the true fluorescence change of one channel protein (theoretical limit).

APPENDIX B: EFFECT OF ACCESS RESISTANCE ON THE MEMBRANE VOLTAGE

In TIR experiments only membrane in close proximity to the glass surface is excited by considerable light intensities. Depending on the distance between the membrane and the surface a non-negligible electrical access resistance R_L may occur. In case the membrane ''seals'' to the surface, this resistance may increase to several $G\Omega$. The resistance will be a function of the distance from the center of the cell and the height of the cleft between glass and membrane. As a result of R_L, a voltage drop over the access resistance will occur, reducing the true membrane potential. As long as the access resistance is much smaller than the membrane resistance R_m, the membrane voltage at this position will reach the applied voltage V_C. In this case, the maximal dF/F of a voltage-dependent dye will not change; the fluorescence signal will merely be very slow ($\tau = R_L C_m$). If R_L and R_m are of comparable size, the voltage will be significantly decreased. The value V_m will be reduced by a factor $R_m/(R_m + R_L)$, thus approaching 0 mV if R_L becomes very large. In Fig. 11, the expected fluorescence signals of a voltage-sensitive dye at a specific spot within the depicted region are illustrated. The overall fluorescence signal would be the integrated fluorescence signal over the detection area.

Sealing of the membrane within the radius r_1 from the center of the cell would result in a normalized fluorescence change of

$$\frac{dF}{F} = \frac{dF}{F_{Ch}} \times \frac{F_{Ch}}{F_{Ch} + F_P + F_B} \times \frac{r_1^2}{r_{det}^2}, \qquad (3)$$

where r_{det} is the radius of the detectable area, assuming the transition from sealed to well-clamped area is very small.

REFERENCES

Asamoah, O. K., J. P. Wuskell, L. M. Loew, and F. Bezanilla. 2003. A fluorometric approach to local electric field measurements in a voltage-gated ion channel. *Neuron.* 37:85–97.

Axelrod, D., E. H. Hellen, and R. M. Fulbright. 1992. Total internal reflection fluorescence. *In* Topics in Fluorescence Spectroscopy. J. R. Lakowicz, editor. Plenum Press, New York.

Blaustein, R. O., P. A. Cole, C. Williams, and C. Miller. 2000. Tethered blockers as molecular ''tape measures'' for a voltage-gated K$^+$ channel. *Nat. Struct. Biol.* 7:309–311.

Braun, D., and P. Fromherz. 1998. Fluorescence interferometry of neuronal cell adhesion on microstructured silicon. *Phys. Rev. Lett.* 81:5241–5244.

Burke, N. A., K. Takimoto, D. Li, W. Han, S. C. Watkins, and E. S. Levitan. 1999. Distinct structural requirements for clustering and immobilization of K$^+$ channels by PSD-95. *J. Gen. Physiol.* 113:71–80.

Cha, A., and F. Bezanilla. 1997. Characterizing voltage-dependent conformational changes in the *Shaker* K$^+$ channel with fluorescence. *Neuron.* 19:1127–1140.

Cha, A., and F. Bezanilla. 1998. Structural implications of fluorescence quenching in the *Shaker* K$^+$ channel. *J. Gen. Physiol.* 112:391–408.

Cha, A., P. C. Ruben, A. L. George, Jr., E. Fujimoto, and F. Bezanilla. 1999a. Voltage sensors in domains III and IV, but not I and II, are immobilized by Na$^+$ channel fast inactivation. *Neuron.* 22:73–87.

Cha, A., G. E. Snyder, P. R. Selvin, and F. Bezanilla. 1999b. Atomic scale movement of the voltage-sensing region in a potassium channel measured via spectroscopy. *Nature*. 402:809–813.

Chahine, M., P. B. Bennett, A. L. George, Jr., and R. Horn. 1994. Functional expression and properties of the human skeletal muscle sodium channel. *Pflugers Arch*. 427:136–142.

Chanda, B., and F. Bezanilla. 2002. Tracking voltage-dependent conformational changes in skeletal muscle sodium channel during activation. *J. Gen. Physiol*. 120:629–645.

Gandhi, C. S., E. Clark, E. Loots, A. Pralle, and E. Y. Isacoff. 2003. The orientation and molecular movement of a K^+ channel voltage-sensing domain. *Neuron*. 40:515–525.

Gandhi, C. S., E. Loots, and E. Y. Isacoff. 2000. Reconstructing voltage sensor-pore interaction from a fluorescence scan of a voltage-gated K^+ channel. *Neuron*. 27:585–595.

Geibel, S., J. H. Kaplan, E. Bamberg, and T. Friedrich. 2003a. Conformational dynamics of the Na^+/K^+-ATPase probed by voltage clamp fluorometry. *Proc. Natl. Acad. Sci. USA*. 100:964–969.

Geibel, S., D. Zimmermann, G. Zifarelli, A. Becker, J. B. Koenderink, Y. K. Hu, J. H. Kaplan, T. Friedrich, and E. Bamberg. 2003b. Conformational dynamics of Na^+/K^+- and H^+/K^+-ATPase probed by voltage clamp fluorometry. *Ann. N. Y. Acad. Sci*. 986:31–38.

Glauner, K. S., L. M. Mannuzzu, C. S. Gandhi, and E. Y. Isacoff. 1999. Spectroscopic mapping of voltage sensor movement in the *Shaker* potassium channel. *Nature*. 402:813–817.

Gonzalez, C., E. Rosenman, F. Bezanilla, O. Alvarez, and R. Latorre. 2000. Modulation of the *Shaker* K^+ channel gating kinetics by the S3–S4 linker. *J. Gen. Physiol*. 115:193–208.

Gonzalez, C., E. Rosenman, F. Bezanilla, O. Alvarez, and R. Latorre. 2001. Periodic perturbations in *Shaker* K^+ channel gating kinetics by deletions in the S3–S4 linker. *Proc. Natl. Acad. Sci. USA*. 98:9617–9623.

Jiang, Y., A. Lee, J. Chen, V. Ruta, M. Cadene, B. T. Chait, and R. MacKinnon. 2003a. X-ray structure of a voltage-dependent K^+ channel. *Nature*. 423:33–41.

Jiang, Y., V. Ruta, J. Chen, A. Lee, and R. MacKinnon. 2003b. The principle of gating charge movement in a voltage-dependent K^+ channel. *Nature*. 423:42–48.

Jugloff, D. G., R. Khanna, L. C. Schlichter, and O. T. Jones. 2000. Internalization of the Kv1.4 potassium channel is suppressed by clustering interactions with PSD-95. *J. Biol. Chem*. 275:1357–1364.

Lakowicz, J. R. 1999. Principles of Fluorescence Spectroscopy. Kluwer Academic/Plenum Publishers, New York.

Larsson, H. P., O. S. Baker, D. S. Dhillon, and E. Y. Isacoff. 1996. Transmembrane movement of the *Shaker* K^+ channel S4. *Neuron*. 16:387–397.

Li, M., R. A. Farley, and H. A. Lester. 2000. An intermediate state of the gamma-aminobutyric acid transporter GAT1 revealed by simultaneous voltage clamp and fluorescence. *J. Gen. Physiol*. 115:491–508.

Li, M., and H. A. Lester. 2002. Early fluorescence signals detect transitions at mammalian serotonin transporters. *Biophys. J*. 83:206–218.

Loew, L. M. 1982. Design and characterization of electrochromic membrane probes. *J. Biochem. Biophys. Methods*. 6:243–260.

Loo, D. D., B. A. Hirayama, E. M. Gallardo, J. T. Lam, E. Turk, and E. M. Wright. 1998. Conformational changes couple Na^+ and glucose transport. *Proc. Natl. Acad. Sci. USA*. 95:7789–7794.

Mannuzzu, L. M., and E. Y. Isacoff. 2000. Independence and cooperativity in rearrangements of a potassium channel voltage sensor revealed by single subunit fluorescence. *J. Gen. Physiol*. 115:257–268.

Mannuzzu, L. M., M. M. Moronne, and E. Y. Isacoff. 1996. Direct physical measure of conformational rearrangement underlying potassium channel gating. *Science*. 271:213–216.

Mathur, R., J. Zheng, Y. Yan, and F. J. Sigworth. 1997. Role of the S3–S4 linker in *Shaker* potassium channel activation. *J. Gen. Physiol*. 109: 191–199.

Meinild, A. K., B. A. Hirayama, E. M. Wright, and D. D. Loo. 2002. Fluorescence studies of ligand-induced conformational changes of the Na^+/glucose cotransporter. *Biochemistry*. 41:1250–1258.

Ren, D., B. Navarro, H. Xu, L. Yue, Q. Shi, and D. E. Clapham. 2001. A prokaryotic voltage-gated sodium channel. *Science*. 294:2372–2375.

Riven, I., E. Kalmanzon, L. Segev, and E. Reuveny. 2003. Conformational rearrangements associated with the gating of the G protein-coupled potassium channel revealed by FRET microscopy. *Neuron*. 38:225–235.

Schonherr, R., L. M. Mannuzzu, E. Y. Isacoff, and S. H. Heinemann. 2002. Conformational switch between slow and fast gating modes: allosteric regulation of voltage sensor mobility in the EAG K^+ channel. *Neuron*. 35:935–949.

Schwarz, T. L., B. L. Tempel, D. M. Papazian, Y. N. Jan, and L. Y. Jan. 1988. Multiple potassium-channel components are produced by alternative splicing at the *Shaker* locus in *Drosophila*. *Nature*. 331:137–142.

Shoeb, F., A. P. Malykhina, and H. I. Akbarali. 2003. Cloning and functional characterization of the smooth muscle ether-a-go-go-related gene K^+ channel. Potential role of a conserved amino acid substitution in the S4 region. *J. Biol. Chem*. 278:2503–2514.

Smith, P. L., and G. Yellen. 2002. Fast and slow voltage sensor movements in HERG potassium channels. *J. Gen. Physiol*. 119:275–293.

Sonnleitner, A., L. M. Mannuzzu, S. Terakawa, and E. Y. Isacoff. 2002. Structural rearrangements in single ion channels detected optically in living cells. *Proc. Natl. Acad. Sci. USA*. 99:12759–12764.

Sørensen, J. B., A. Cha, R. Latorre, E. Rosenman, and F. Bezanilla. 2000. Deletion of the S3–S4 linker in the *Shaker* potassium channel reveals two quenching groups near the outside of S4. *J. Gen. Physiol*. 115:209–222.

Sund, S. E., and D. Axelrod. 2000. Actin dynamics at the living cell submembrane imaged by total internal reflection fluorescence photobleaching. *Biophys. J*. 79:1655–1669.

Tang, C. Y., and D. M. Papazian. 1997. Transfer of voltage independence from a rat olfactory channel to the *Drosophila* ether-a-go-go K^+ channel. *J. Gen. Physiol*. 109:301–311.

Vilardaga, J. P., M. Bunemann, C. Krasel, M. Castro, and M. J. Lohse. 2003. Measurement of the millisecond activation switch of G protein-coupled receptors in living cells. *Nat. Biotechnol*. 21:807–812.

Zheng, J., and W. N. Zagotta. 2000. Gating rearrangements in cyclic nucleotide-gated channels revealed by patch-clamp fluorometry. *Neuron*. 28:369–374.